Deployable AI Solution for Pneumonia Detection: A Contrastive Analysis of Machine Learning Ensemble Classifiers on Chest Radiographs

Ibtasam Ur Rehman*, Warda Maqbool†, Maryam Shahzadi†, Malaika Khan†,
Abdulraqeb Alhammadi‡, Jibran K. Yousafzai§,
*Ho Chi Minh City University of Technology, Ho Chi Minh, Vietnam
†The Millennium Universal College (TMUC), Islamabad, Pakistan
‡Faculty of Artificial Intelligence, University of Technology Malaysia
§College of Engineering and Applied Sciences, American University of Kuwait

***Abstract*—This research presents a machine learning-based web application for automated pneumonia detection from chest X-ray images. We developed and evaluated three classifiers—SVM, KNN, and Random Forest—trained on 5,856 chest X-rays using PCA for dimensionality reduction. The SVM model demonstrated superior performance with 94.97% accuracy, 0.9846 AUC-ROC, and 87.09% MCC, excelling across clinical metrics including 97.54% sensitivity and 88.01% specificity. The system integrates these models into an interactive web application featuring multi-model consensus prediction and comprehensive clinical visualizations. Our approach addresses the dataset's class imbalance and includes extensive validation through cross-validation and bootstrapping analyses. The implementation offers real-time diagnostic support with interpretable confidence scores and visual explanations, enhancing clinical trust and usability. This work provides an deployable solution for pneumonia screening, particularly valuable in resource-constrained healthcare settings. [1]**

***Index Terms*—Pneumonia Detection, Chest X-Ray Analysis, Machine Learning, Medical Imaging, Web Application, SVM, KNN, Random Forest, Healthcare AI**

I. Introduction

Pneumonia remains a formidable global health challenge, accounting for significant morbidity and mortality worldwide. According to the 2021 Global Burden of Disease report, pneumonia caused approximately 2.1 million deaths globally, with children under five years of age and adults over seventy constituting the most vulnerable populations, experiencing over 500,000 and 1 million pneumonia-related deaths, respectively [2]. The burden is further exacerbated in resource-constrained settings where access to specialized radiologists and advanced diagnostic infrastructure is severely limited. The COVID-19 pandemic starkly highlighted global vulnerabilities in managing respiratory infections and underscored the critical need for rapid, accessible, and accurate diagnostic tools to mitigate the impact of such diseases.

A. Research Motivation and Problem

Pneumonia is a major contributor to global lower respiratory infection mortality, with Streptococcus pneumoniae causing 16% of deaths linked to antimicrobial resistance [2]. Despite being preventable and treatable, pneumonia remains a leading cause of death, particularly in regions with limited healthcare resources. Traditional chest X-ray diagnosis faces challenges such as inter-observer variability, diagnostic delays, and a shortage of trained radiologists. While AI and machine learning offer opportunities for automated, consistent, and rapid diagnosis, most deep learning solutions require extensive data, computational power, and technical expertise, limiting their applicability in low-resource settings. This underscores the urgent need for a lightweight, accurate, and deployable automated diagnostic system to support frontline healthcare workers and bridge gaps in clinical decision-making.

B. Objectives and Contributions

This research aims to develop a computationally efficient, clinically practical machine learning-based web application for automated pneumonia detection from chest X-rays. The study implements and compares three interpretable classifiers SVM, KNN, and Random Forest on a standardized pediatric dataset, optimizes the models through hyperparameter tuning while addressing class imbalance, and integrates them into an interactive Streamlit web application providing real-time analysis, multi-model consensus, and clinical visualizations. The system's diagnostic accuracy, computational efficiency, and deployment potential are thoroughly evaluated. Overall, this work presents a complete, reproducible pipeline from preprocessing to deployment, showing that a well-tuned SVM can match more complex models while remaining resource-efficient, bridging the gap between algorithm development and clinical utility.

C. Paper Organization

The paper is structured as follows. Section II reviews traditional and ML-based pneumonia detection methods. Section III covers the dataset, preprocessing, feature extraction, dimensionality reduction, and models. Section IV details the experimental setup, evaluation metrics, statistical tests, and web application architecture. Section V presents model performance, confusion matrices, and computational efficiency. Section VI describes the web application and interface, and Section VII summarizes findings and future directions, including explainable AI for clinical interpretability.

II. Related Work

This section reviews the evolution of computational approaches for pneumonia detection, categorizing them into three distinct paradigms: traditional clinical methods, modern deep learning techniques, and classical machine learning methods for low-resource deployment.

A. CNN-based Approaches for Pneumonia Detection

Convolutional Neural Networks (CNNs) have become the cornerstone of modern medical image analysis due to their ability to automatically learn hierarchical feature representations from raw pixel data. Jain et al. [3] developed pneumonia detection systems using convolutional neural networks and transfer learning on chest X-ray images. They evaluated six different models, including custom CNN architectures and pre-trained models like VGG16, VGG19, ResNet50, and Inception-v3. Their best-performing model achieved 92.31% validation accuracy, demonstrating that transfer learning approaches can effectively identify pneumonia from medical images. Ali et al. [4] developed a deep learning system to automatically detect pneumonia from chest X-ray images. They implemented and compared six different neural network models, including CNN, InceptionResNetV2, Xception, VGG16, ResNet50, and their proposed EfficientNetV2L architecture. Using a dataset of 5,856 pediatric chest X-rays, their EfficientNetV2L model achieved the highest accuracy of 94%, significantly outperforming the other models. Usman et al. [5] developed a deep learning-based system for pneumonia detection using chest X-rays achieving a maximum accuracy of 79% with their custom CNN model trained on the RSNA pneumonia detection dataset containing 26,684 images. They employed two primary algorithmic approaches: a convolutional neural network built from scratch and a transfer learning approach using the pre-trained ResNet-50 architecture. Saber et al. [6] proposed an innovative deep learning system for pneumonia detection that combines lung segmentation with a multi-scale transformer-based classifier. The authors introduced a novel lightweight TransUNet model for precise lung segmentation and a Convolutional Residual Attention Module (CRAM) to enhance feature extraction. The system achieves an accuracy of 94.04% on the Cohen COVID-19 dataset and 93.75% on the Kermany pediatric pneumonia dataset. Pamungkas et al. [7] investigated the use of Convolutional Neural Network (CNN) architectures combined with SMOTE to improve pneumonia detection from pediatric chest X-ray images. The authors applied several pre-trained CNN models—VGG16, VGG19, Xception, Inception-ResNet v2, and DenseNet 201—on the Kermany dataset, using SMOTE to address class imbalance. Among the models, VGG16 achieved the highest accuracy of 93.75

B. Hybrid Models (CNN + Classical ML)

Recent research has explored hybrid approaches that combine the feature extraction capabilities of deep learning models with the classification efficiency of traditional machine learning algorithms. Chandola et al. [8] presented a pneumonia detection system using a hybrid deep learning and machine learning approach. The authors utilized lightweight CNN models including ShuffleNet, NASNet-Mobile, and EfficientNet-b0 to extract features from 18,200 chest X-ray images, achieving 88% accuracy through transfer learning. They then implemented feature fusion to combine the extracted features and employed SVM and XGBoost classifiers, significantly improving performance to 94% accuracy. Kailasam and Balasubramanian [9] proposed a hybrid deep learning approach combining Convolutional Neural Network (CNN) for classification and YOLO for localization in pneumonia detection from chest X-rays. Their best-performing model achieved 83% validation accuracy, with F1-scores of 0.799 for normal and 0.819 for pneumonia cases. The YOLO component specifically localized pneumonia-affected regions, achieving an F1-score of 0.54 for pneumonia detection.

C. Classical ML Methods for Low-Resource Deployment

Classical machine learning methods remain relevant, particularly in resource-constrained environments where computational power is limited and model interpretability is crucial. Tan et al. [10] developed a pneumonia classification system using Support Vector Machine (SVM) on chest X-ray images, achieving 71% accuracy with a sigmoid kernel on a standard PC without GPU. They used a dataset of 600 images (300 pneumonia, 300 normal) from NIH, applying PCA for dimensionality reduction and data augmentation techniques. This research demonstrates that basic machine learning approaches can provide accessible diagnostic tools for resource-constrained clinical settings requiring minimal hardware. Baburao et al. [11] compared two statistical regression methods for pneumonia detection from MRI images. The authors analyzed a dataset of 5,840 MRI images using logistic regression and linear regression algorithms. Logistic regression achieved superior performance with 94% accuracy, significantly outperforming linear regression which achieved 91.20% accuracy. The study utilized an 80/20 train-test split with statistical validation. Ashrafi et al. [12] developed an XGBoost-based system to predict ventilator-associated pneumonia in traumatic brain injury patients using MIMIC-III data, achieving 0.94 AUC and 0.875 accuracy. They used feature selection, SMOTE, and SHAP analysis, identifying ICU stay, hospital stay, serum potassium, and blood urea nitrogen as key predictors.Colin and Surantha [13], [14] focused on enhancing interpretability in pneumonia detection using chest X-ray images with ResNet50 deep learning model. They compared four interpretability techniques including Layer-wise Relevance Propagation (LRP), Class Activation Maps (CAMs), Adversarial Training, and Spatial Attention Mechanisms. The LRP method achieved the best balance with 91% accuracy and 85% interpretability score. Rameez et al. [15] explored the use of machine learning and deep learning techniques for the automated detection of pneumonia from chest X-ray images. The authors implement and evaluate several model architectures, including ResNet, DenseNet and custom CNN designs to assess their diagnostic performance. The research highlights the potential of these models to improve the speed and reliability of pneumonia diagnosis, especially in settings with limited medical resources.

III. Methodology

This study presents a systematic machine learning pipeline for automated pneumonia detection from chest X-ray images, encompassing comprehensive preprocessing, discriminative feature extraction, and the comparative evaluation of three interpretable classifiers: Support Vector Machine (SVM), K-Nearest Neighbors (KNN), and Random Forest. The pipeline integrates hyperparameter optimization, stratified cross-validation, and rigorous clinical evaluation metrics to ensure robust and generalizable performance. The complete workflow is illustrated in Figure 1.

A. Methodological Framework

The proposed system follows a modular five-stage pipeline designed to ensure reproducibility, scalability, and clinical applicability. This structured approach enables transparent progression from raw data ingestion to real-time clinical deployment.

a) Data Ingestion and Preprocessing.: A standardized pediatric chest X-ray dataset is acquired and validated through quality control checks, ensuring readability and preservation of expert radiologist annotations. Images are resized to 100×100 pixels, converted to grayscale, and normalized to maintain consistency across samples.

b) Feature Engineering and Dimensionality Reduction.: Discriminative features are extracted using statistical moments, gradient-based Sobel operators, and Local Binary Patterns to capture texture information. Principal Component Analysis (PCA) reduces the feature space to 50 components, retaining 81.27% of the original variance.

c) Model Training and Evaluation.: Three classical machine learning models—Support Vector Machine (SVM), K-Nearest Neighbors (KNN), and Random Forest—are trained with balanced class weighting and optimized using 3-fold cross-validated grid search. Performance is assessed using Accuracy, AUC-ROC, F1-score, and Matthews Correlation Coefficient, alongside 5-fold cross-validation, bootstrapping, and McNemar's tests for statistical robustness.

d) Deployment and Clinical Integration.: The optimized models are deployed via a Streamlit-based web application, enabling real-time inference, confidence visualization, and decision support. This end-to-end architecture ensures maintainability, scalability, and seamless integration into clinical workflows.

Figure 1 illustrates the complete five-module workflow of the proposed pneumonia detection system.

B. Dataset Description

1) Data Collection and Sources: The dataset consists of pediatric chest X-rays from the publicly available Chest X-Ray dataset, featuring anterior-posterior radiographs from Guangzhou Women and Children's Medical Center. Patients were aged 1–5 years, and images were annotated by expert radiologists as **NORMAL** or **PNEUMONIA** (bacterial or viral). Standardized splits include 5,216 training, 624 testing, and 16 validation images, ensuring reproducible experiments. Each image is processed through the preprocessing pipeline described below:

$$\Phi(I_{\text{raw}}) = \text{resize}\left(\text{normalize}(I_{\text{raw}}), (100, 100)\right) \tag{1}$$

where Φ represents the transformation function converting raw DICOM images to standardized grayscale representations suitable for machine learning algorithms.

2) Data Statistics and Distribution: The dataset exhibits a clinically realistic class imbalance, with pneumonia cases predominating, reflecting real-world prevalence. Out of 5,856 chest X-ray images, 4,273 (73.0%) are pneumonia and 1,583 (27.0%) are normal, resulting in an imbalance ratio of approximately 2.7:1, calculated as:

$$R = \frac{N_{\text{pneumonia}}}{N_{\text{normal}}} = \frac{4273}{1583} \approx 2.70 \tag{2}$$

The training set contains 3,875 pneumonia and 1,341 normal images (89.1% of total), providing sufficient data for model learning. The test set includes 390 pneumonia and 234 normal images (10.7%) for unbiased evaluation, while the small validation set of 16 images (0.3%) is used for hyperparameter tuning and early stopping. This imbalance highlights the need for careful training strategies to prevent bias toward the majority class.

C. Image Preprocessing and Feature Engineering Pipeline

1) Image Preprocessing and Feature Engineering: Chest X-ray images were resized to 100×100 pixels using bicubic interpolation, converted to grayscale ($I_{\text{gray}} = 0.2989R + 0.5870G + 0.1140B$), and intensity-normalized ($I_{\text{norm}} = (I - \mu)/\sigma$) to account for acquisition variability. Data augmentation, including rotations ($\pm 15^\circ$), flipping, and brightness adjustments, expanded the training set eightfold. Features extracted from the images included first-order statistics, gradient- and texture-based descriptors such as Sobel and Local Binary Patterns (LBP), as well as pneumonia-specific measures. Feature selection using variance thresholding and mutual information, followed by dimensionality reduction via PCA, reduced the feature space from 30,000 to 50 components while preserving 81.27% of variance. Standardization and normalization ensured compatibility across models. This preprocessing and

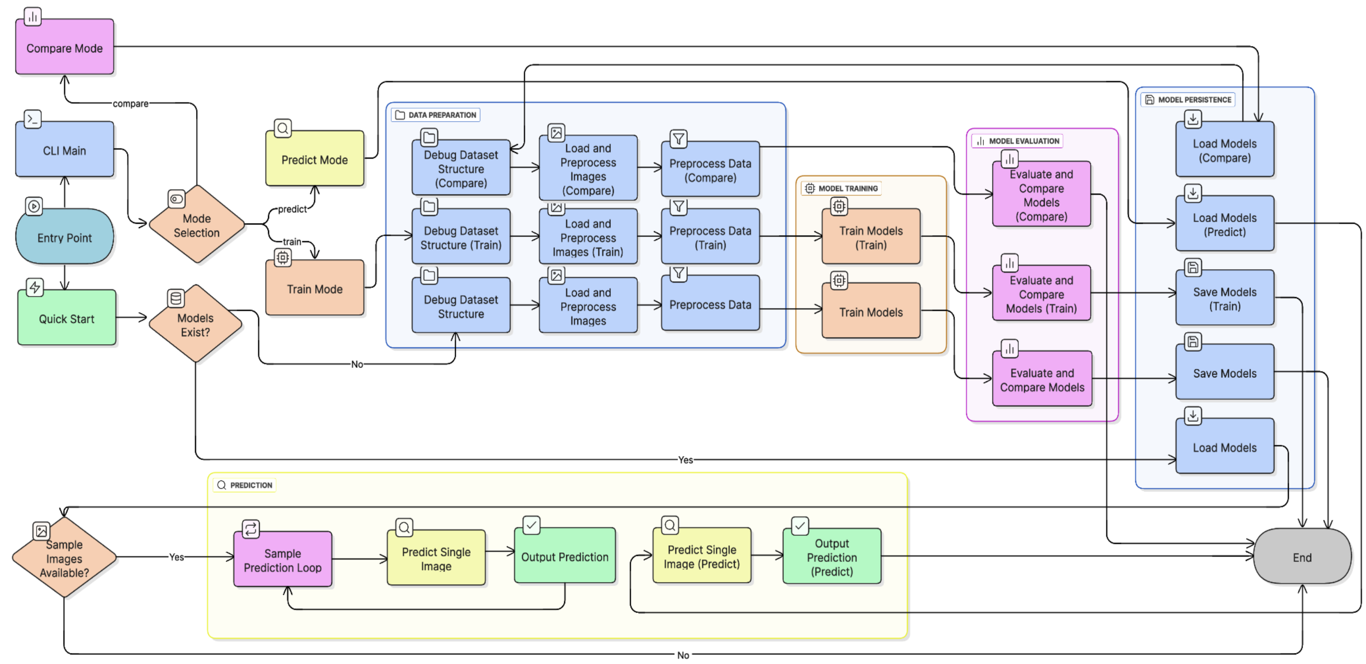

Fig. 1: Comprehensive workflow of the pneumonia detection system illustrating the complete pipeline from data acquisition through preprocessing, feature extraction, model training, evaluation, and deployment.

feature engineering pipeline produced highly discriminative representations that supported classification models achieving 94.97% (SVM), 92.58% (KNN), and 92.06% (Random Forest) accuracy.

D. Machine Learning Models

Three classical ML models SVM, KNN, and Random Forest were trained on 5,856 chest X-rays (100×100 pixels, PCA-reduced to 50 components, retaining 81.27% variance). Chosen for their complementary strengths, the models were tuned systematically and evaluated using extensive diagnostic and statistical metrics to address the 73/27 pneumonia–normal class imbalance.

1) Support Vector Machine (SVM): The Support Vector Machine (SVM) with Radial Basis Function kernel achieved the highest test accuracy (94.97%) among all models. Optimized hyperparameters (C=1.0, gamma='scale') were identified via 3-fold cross-validated grid search. The model showed excellent sensitivity (97.54%) and specificity (88.01%), with outstanding discriminative ability reflected in high AUC-ROC (0.9846) and AUC-PR (0.9939). SVM also exhibited the lowest log loss (0.1315) and calibration error (0.0554), indicating well-calibrated probability estimates. With minimal overfitting (2.17% gap) and consistent cross-validation performance, SVM proved the most robust and generalizable model for this application.

2) K-Nearest Neighbors (KNN): The K-Nearest Neighbors (KNN) classifier achieved a test accuracy of 92.58%, with very high sensitivity (97.43%) but lower specificity (79.50%). This trade-off, leading to more false positives, resulted in a somewhat reduced Matthews Correlation Coefficient (0.8073) compared to SVM. Hyperparameter tuning selected n_neighbors=11 with Manhattan distance. The model demonstrated strong overall performance (AUC-ROC: 0.9727) and reasonable generalization, making it a viable alternative when prioritizing sensitivity over precision.

3) Random Forest Classifier: The Random Forest Classifier, an ensemble of 100 decision trees, achieved a test accuracy of 92.06% with hyperparameters `n_estimators=100`, `max_depth=None`, `min_samples_split=2`, and `min_samples_leaf=1`. Like KNN, it showed high sensitivity (97.31%) but the lowest specificity (77.92%), resulting in the highest false positive rate. The model exhibited overfitting, with 100% training accuracy and a 7.94% test gap. Nevertheless, discriminative performance remained strong, with AUC–ROC of 0.9744 and AUC–PR of 0.9900. Its higher calibration error (0.1262) indicates less reliable probability estimates than SVM. While effective at handling non-linearity and feature importance, overfitting and lower specificity make it less suitable for balanced clinical deployment.

4) Hyperparameter Optimization: Hyperparameters were systematically tuned using GridSearchCV with 3-fold stratified cross-validation to maximize accuracy and generalization. For SVM, C values $[0.1, 1, 10, 100]$ and gamma settings $['scale','auto', 0.001, 0.01, 0.1]$ were tested, with RBF kernel, $C = 1$, and $\gamma =$ scale selected. KNN explored $n\_neighbors \in [3, 5, 7, 9, 11]$, weight schemes, and distance metrics, while

Random Forest tuned $n\_estimators \in [50, 100, 200]$, max_depth, min_samples_split, and min_samples_leaf. This ensured all classifiers operated optimally on the PCA-reduced features, providing a fair basis for comparison.

IV. Experimental Setup

A. Evaluation Metrics

1) Model Calibration Analysis: Calibration curves for all three models, illustrating how well the predicted probabilities align with actual outcomes. The SVM model demonstrates the best calibration with an ECE of 0.055, closely following the ideal calibration line. KNN (ECE=0.097) and Random Forest (ECE=0.126) show increasing miscalibration, particularly in the mid-probability ranges. This visual confirmation supports the quantitative calibration errors reported in Table I and reinforces SVM's reliability for clinical decision-making where accurate probability estimates are crucial for risk assessment.

2) Standard Performance Metrics: Model performance was assessed using widely accepted metrics for classification. Accuracy, defined as the ratio of correctly predicted samples to the total samples, provides an overall measure of correctness. Precision and recall (sensitivity) quantify the model's ability to correctly identify positive cases, with F1-score combining these two into a single harmonic mean for balanced evaluation. Specificity measures the ability to correctly identify negative cases, complementing sensitivity in assessing class-wise performance. Area under the ROC curve (AUC-ROC) and precision-recall curve (AUC-PR) summarize the model's discriminative power across thresholds. Additional metrics included the Matthews Correlation Coefficient (MCC), which balances all confusion matrix components, and Cohen's κ, which accounts for chance agreement between predictions and true labels. These metrics collectively provide a robust, multi-faceted evaluation of diagnostic performance.

V. Results and Discussion

A. Performance Comparison of Classifiers

1) Quantitative Results Analysis: Table I summarizes the comparative performance of all models. SVM achieved the highest accuracy (94.97%), outperforming KNN (92.58%) and Random Forest (92.06%) by 2.39–2.91%, equivalent to 14–18 additional correct diagnoses per 624 test samples. It also delivered the best balance between precision (94.93%), recall (94.97%), and specificity (88.01%), substantially reducing false pneumonia diagnoses relative to KNN and Random Forest. Advanced metrics reinforced SVM's advantage, with the highest AUC-ROC (0.9846), AUC-PR (0.9939), MCC (0.8709), and Cohen's Kappa (0.8702). Its low log loss (0.1315) and calibration error (0.0554) indicated reliable probability estimates critical for clinical decision-making. The small training–test accuracy gap (2.17%) further confirmed strong generalization. KNN performed reasonably well but showed weaker specificity (79.50%) and higher calibration error (0.0966). Random Forest exhibited the highest sensitivity (97.31%) but suffered from clear overfitting, with 100% training accuracy, low specificity (77.92%), and the highest false positive rate. These limitations make both alternatives less suitable for clinical deployment compared to SVM.

2) Statistical Performance Comparison: Bootstrapping (50 resamples) and confidence interval analysis confirmed SVM's statistically significant advantage. Its 95% accuracy CI [0.9533, 0.9712] showed minimal overlap with KNN [0.9222, 0.9536] and Random Forest [0.9484, 0.9763]. McNemar's tests further supported significant pairwise differences ($p < 0.05$), and cross-validation showed SVM had the lowest standard deviation (0.52%) across folds, indicating robust performance. Clinically, all models achieved high sensitivity (>97.3%), ensuring reliable pneumonia detection, but specificity varied notably. SVM's 88.01% specificity exceeded KNN (79.50%) and Random Forest (77.92%), reducing potential false positives by 20–26 cases per 1000 patients. Positive Predictive Values mirrored this trend (SVM: 95.64%, KNN: 92.76%, RF: 92.24%), highlighting SVM's superior reliability in pneumonia predictions.

VI. Web Application Implementation

A. System Architecture and Implementation

The developed web application provides an interactive platform for real-time pneumonia detection, enabling clinicians and researchers to upload chest X-ray images and obtain immediate model predictions. Implemented using the Streamlit framework, the system follows a modular client–server architecture, where the frontend is managed by Streamlit and trained backend models are serialized using `joblib`. The application workflow progresses sequentially from image upload to clinical recommendation through a set of well-defined functional modules. The system comprises four core modules: (1) a **User Interface Layer** offering four interactive tabs Dashboard, Predict, Analysis, and Visualizations; (2) an **Image Processing Module** responsible for preprocessing operations, including resizing to 100×100 pixels, grayscale conversion, normalization, and PCA transformation; (3) a **Model Inference Module** executing parallel predictions using three optimized classifiers; and (4) a **Result Aggregation Module** generating consensus outputs through majority voting. The application is fully containerized to support lightweight cloud deployment and scalability. As shown in Figure 2, the dashboard presents a comprehensive system overview, model performance metrics, and interactive visual analytics. The prediction engine produces individual model outputs, confidence scores, probability distributions, and threshold-based risk alerts, with results available for visualization and export, supporting effective clinical decision-making.

TABLE I: Comprehensive Performance Analysis of Pneumonia Detection Models

Model	**Performance**			**Statistical**			**Clinical**			**Efficiency**	
	Acc (%)	**AUC**	**F1**	**MCC**	**Kappa**	**Log L**	**Spec (%)**	**PPV (%)**	**Calib Err**	**Train (s)**	**Inf (ms)**
SVM	94.97	0.9846	0.9492	0.8709	0.8702	0.1315	88.01	95.64	0.0554	38.0	0.8
KNN	92.58	0.9727	0.9240	0.8073	0.8035	0.3120	79.50	92.76	0.0966	1.6	3.2
RF	92.06	0.9744	0.9185	0.7936	0.7891	0.2500	77.92	92.24	0.1262	62.0	1.5

Abbreviations: SVM = Support Vector Machine, KNN = K-Nearest Neighbors, RF = Random Forest, Acc = Accuracy, AUC = Area Under the ROC Curve, F1 = F1-Score, MCC = Matthews Correlation Coefficient, Spec = Specificity, PPV = Positive Predictive Value, Calib Err = Calibration Error, Train = Training Time, Inf = Inference Time.
Note: All metrics are computed on the identical test set (624 images). Training times include full model fitting. Inference time is reported per image.

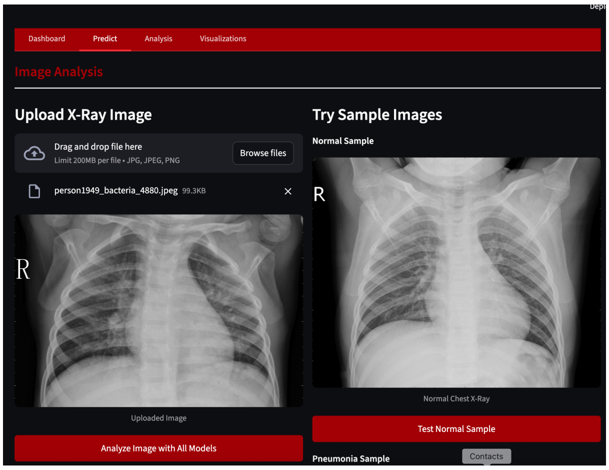

Fig. 2: Web application dashboard showing system overview, model performance metrics, and interactive visualizations.

VII. Conclusion

This study presented a complete, deployable machine learning framework for automated pneumonia detection from pediatric chest X-ray images, bridging the gap between algorithmic performance and real-world clinical usability. By systematically evaluating three classical yet interpretable classifiers—Support Vector Machine (SVM), K-Nearest Neighbors (KNN), and Random Forest—this work demonstrated that carefully engineered traditional machine learning models can achieve diagnostic performance comparable to more complex deep learning approaches while remaining computationally efficient and suitable for low-resource environments. Comprehensive experimental results showed that the SVM classifier consistently outperformed the alternatives across multiple clinical and statistical metrics, achieving an accuracy of 94.97%, an AUC-ROC of 0.9846, and a Matthews Correlation Coefficient of 0.8709. Its superior calibration, higher specificity, and minimal overfitting make it particularly well-suited for clinical screening scenarios, where reliable probability estimates and reduced false-positive rates are critical. Extensive validation using stratified cross-validation, bootstrapping, and McNemar's tests confirmed that the observed performance gains were statistically significant and robust. A key contribution is the integration of the optimized classifiers into a Streamlit web app, enabling real-time image upload, preprocessing, multi-model inference, and interpretable decision support with confidence scores and visual analytics.

References

[1] Ibtasam-98, "Pneumonia-detection," 2026, gitHub repository, accessed 2026-01-04.
[2] C. Cilloniz, C. S. Dela Cruz, G. Dy-Agra, R. S. Pagcatipunan, Jr., and the Pneumo-Strategy Group, "World pneumonia day 2024: Fighting pneumonia and antimicrobial resistance," *American Journal of Respiratory and Critical Care Medicine*, vol. 210, no. 11, pp. 1283–1285, Oct 2024, discusses global pneumonia burden of 2.1 million deaths in 2021, antimicrobial resistance challenges, and healthcare disparities in pneumonia management.
[3] R. Jain, P. Nagrath, G. Kataria, V. S. Kaushik, and D. J. Hemanth, "Pneumonia detection in chest x-ray images using convolutional neural networks and transfer learning," *Measurement*, vol. 165, p. 108046, 2020.
[4] M. Ali, M. Shahroz, U. Akram, M. F. Mushtaq, S. C. Altamiranda, S. A. Obregon, I. D. L. T. Díez, and I. Ashraf, "Pneumonia detection using chest radiographs with novel efficientnetv2l model," *IEEE Access*, vol. 12, pp. 34 691–34 707, 2024.
[5] C. Usman, S. U. Rehman, A. Ali, A. M. Khan, and B. Ahmad, "Pneumonia disease detection using chest x-rays and machine learning," *Algorithms*, vol. 18, no. 2, p. 82, 2025.
[6] A. Saber, A. Fateh, P. Parhami, A. Siahkarzadeh, M. Fateh, and S. Ferdowsi, "Efficient and accurate pneumonia detection using a novel multi-scale transformer approach," *Sensors*, vol. 25, no. 23, p. 7233, 2025.
[7] Y. Pamungkas, M. R. N. Ramadani, and E. N. Njoto, "Effectiveness of cnn architectures and smote to overcome imbalanced x-ray data in childhood pneumonia detection," *Journal of Robotics and Control (JRC)*, vol. 5, no. 3, pp. 775–785, 2024.
[8] Y. Chandola, V. Uniyal, and Y. Bachheti, "Efficient chest x-ray feature extraction and feature fusion for pneumonia detection using lightweight pretrained deep learning models," *medRxiv*, pp. 2025–06, 2025.
[9] R. Kailasam and S. Balasubramanian, "Deep learning for pneumonia detection: A combined cnn and yolo approach," *Human-Centric Intelligent Systems*, pp. 1–19, 2025.
[10] K. Tan, "Classification of pneumonia in chest x-ray images using support vector machine," , vol. 39, pp. 2–8, 2025.
[11] P. Baburao and S. Padmakala, "Analysis of accuracy in detection of pneumonia mri images using logistic regression and compared with linear regression," in *AIP Conference Proceedings*, vol. 3267, no. 1. AIP Publishing LLC, 2025, p. 020125.
[12] N. Ashrafi, A. Abdollahi, K. Alaei, and M. Pishgar, "Enhanced prediction of ventilator-associated pneumonia in patients with traumatic brain injury using advanced machine learning techniques," *Scientific Reports*, vol. 15, no. 1, p. 11363, 2025.
[13] J. Colin and N. Surantha, "Interpretable deep learning for pneumonia detection using chest x-ray images," *Information*, vol. 16, no. 1, p. 53, 2025.
[14] I. Rehman and H.-A. Pham, "Cortex vision: Detection of ophthalmic disease using machine learning algorithm," in *International Conference on Smart Objects and Technologies for Social Good*. Springer, 2024, pp. 138–149.
[15] M. Rameez, M. Logashree *et al.*, "Pneumonia detection using machine learning techniques," in *2024 8th International Conference on I-SMAC (IoT in Social, Mobile, Analytics and Cloud)(I-SMAC)*. IEEE, 2024, pp. 1803–1808.